C(8), C(8)-C(9), C(11)-C(12), C(12)-C(13), and C(13)-C(14) bonds that result in bringing O(33) closer to O(15), O(20), and O(40) and [with a major change in the position of O(43)] produce a very distorted octahedron of oxygen atoms around the sodium ion (18). Therefore, our results show that, unlike the case of neutral depsipeptide valinomycin (19–21), which complexes metals with a greatly changed conformation, the lasalocid molecule undergoes only minor changes in conformation on complex formation to sodium ions. This finding is consistent with results obtained previously for both monensin (22, 23) and grisorixin (24, 25).

The study reported here provides the following important information on lasalocid A. (i) There is no reliable evidence for a conformation of the lasalocid backbone significantly different from the circular one stabilized by hydrogen bonding that has been found in all x-ray studies thus far reported. Crystals obtained from the polar methanol solutions have now been shown also to contain this conformation. (ii) This appears to be the first time that the hydrogen atoms can be clearly recognized from an x-ray study of a lasalocid derivative, and so the hydrogen bonding patterns that were previously inferred are now confirmed. (iii) In contrast to our previous work, the x-ray analysis reveals a lasalocid A monomer (26). That lasalocid and its sodium salt crystallize from methanol solution as monomers is entirely consistent with the NMR results in polar solutions (10), and implies that the form in which lasalocid crystallizes is highly dependent on the species existing in the solution. The existence of monomeric and dimeric structures for lasalocid derivatives under different conditions implies that metal uptake and release in polar environments involve a monomeric form, while transport in nonpolar media takes place by means of a lasalocid dimer (27). This idea can be extended to suggest that the ionophore is a dimer in the lipid bilayer, but reverts to a monomeric structure at the polar exterior.

CHIAN C. CHIANG, IAIN C. PAUL*
Noyes Chemical Laboratory,
University of Illinois, Urbana 61801

References and Notes

1. S. M. Johnson, J. Herrin, S. J. Liu, I. C. Paul, *J. Chem. Soc. Chem. Commun.* (1970), p. 72.
2. ———, *J. Am. Chem. Soc.* 92, 4428 (1970).
3. C. A. Maier and I. C. Paul, *J. Chem. Soc. Chem. Commun.* (1971), p. 181.
4. C. I. Hejna and I. C. Paul, unpublished data.
5. P. G. Schmidt, A. H.-J. Wang, I. C. Paul, *J. Am. Chem. Soc.* 96, 6189 (1974).
6. E. C. Bissell and I. C. Paul, *J. Chem. Soc. Chem. Commun.* (1972), p. 967.
7. In all, 15 crystallographically independent molecules (or anions) of lasalocid A, or of a simple derivative, have been studied in our laboratory. The widest variation of any torsion angle involving only the atoms of the backbone is 26°; many of the variations for a particular backbone torsion angle are less than 15°.
8. A dimeric structure has been found in the case of the Ca²⁺ salt of the acid ionophore, A 23187 [G. D. Smith and W. L. Duax, *J. Am. Chem. Soc.* 98, 1578 (1976)]. However, no examples, other than of lasalocid, are known of dimers with monovalent cations, or of uncharged species.
9. D. J. Patel and C. Shen, *Proc. Natl. Acad. Sci. U.S.A.* 73, 1786 (1976).
10. C. Shen and D. J. Patel, *ibid.*, p. 4277.
11. The form of lasalocid that we present in this report has a ketone stretching frequency at 1722 cm⁻¹. Another crystallographically distinct form of the free acid has been obtained from methanol and has a ketone stretching frequency at 1713 cm⁻¹ (12).
12. J. M. Friedman, D. L. Rousseau, C. Shen, in preparation.
13. The structures were solved and completely refined in the space of 2 to 3 days each on the SYNTEX-EXTL computer system in our laboratory. The structure solutions were effected by a version of MULTAN incorporated in this system.
14. In both crystals, there is slight disorder of the methanol molecule occasioned by libration of the methyl group while the position and direction of the hydrogen-bonded O-H group are preserved. This libration has prevented us from locating the methyl hydrogen atoms with certainty.
15. We have also completed the x-ray analysis of the 1 : 1 complex of 5-bromolasalocid with ethanol. This structure is almost identical, including hydrogen bonding assignments, with that of the 1 : 1 lasalocid : methanol complex described here, and hence it will not be described at this time (C. C. Chiang and I. C. Paul, unpublished data).
16. J. M. Friedman, D. L. Rousseau, C. Shen, I. C. Paul, in preparation.
17. G. D. J. Phillies and H. E. Stanley, *J. Am. Chem. Soc.* 98, 3892 (1976).
18. The "worst" octahedral angles are O(20)-Na-O(31), which is 129.4° (ideal, 180°), and O(20)-Na-O(33), which is 137.3° (ideal, 90°).
19. G. D. Smith, W. L. Duax, D. A. Langs, G. T. DeTitta, J. W. Edmonds, D. C. Rohrer, C. M. Weeks, *J. Am. Chem. Soc.* 97, 7242 (1975).
20. I. L. Karle, *ibid.*, p. 4379.
21. K. Neupert-Laves and M. Dobler, *Helv. Chim. Acta* 58, 432 (1975).
22. M. Pinkerton and L. K. Steinrauf, *J. Mol. Biol.* 49, 533 (1970).
23. W. K. Lutz, F. K. Winkler, J. D. Dunitz, *Helv. Chim. Acta* 54, 1103 (1971).
24. M. Alleaume and D. Hickel, *J. Chem. Soc. Chem. Commun.* (1970), p. 1422; *ibid.* (1972), p. 175.
25. M. Alleaume, *Abstracts of Second European Crystallographic Meeting* (Keszthely, Hungary, 1974), p. 405.
26. It is of considerable interest that the free acid of a bromo derivative of isolasalocid, where the tetrahydropyran ring in lasalocid is replaced by a second tetrahydrofuran ring, has been shown to be monomeric and to exhibit a very different conformation [J. W. Westley, J. F. Blount, R. H. Evans, Jr., A. Stempel, J. Berger, *J. Antibiot.* 27, 597 (1974)].
27. A numbering scheme for lasalocid and other ionophores based on biogenetic arguments has recently been proposed [J. W. Westley, *J. Antibiot.* 29, 584 (1976)]. However, as all the published x-ray data refer to a scheme proposed originally by us, we continue to use that scheme for consistency and ease of comparison among the various compounds studied.
28. This work was supported by NIH grant GM 19336. The SYNTEX x-ray diffractometer and EXTL computer system used in this work were purchased with the aid of NSF equipment grant MPS 75-05911 to the University of Illinois. J. Berger and J. W. Westley of Hoffmann-La-Roche have generously provided us with many samples of lasalocid over the past few years. We have benefited greatly from discussions with Dr. Westley and with D. J. Patel and D. Rousseau of Bell Laboratories. Dr. Rousseau provided us with the crystalline samples used in this study.
* Address correspondence to I.C.P.

29 November 1976; revised 4 February 1977

Anoxic, Hypersaline Basin in the Northern Gulf of Mexico

Abstract. *A 400-square-kilometer depression in the continental slope of the northern Gulf of Mexico (approximately 27°N, 91°W) has been found to contain anoxic, hypersaline (~ 250 grams per kilogram) water in the bottom 200 meters. The interface between the brine and overlying seawater acts as a midwater seismic reflector similar to those seen in the Red Sea. The bulk chemical composition of the brine is similar to that from the Red Sea, but differences between the two in both heat content and geomorphological setting indicate different modes of origin.*

In November 1975, sediment samples were collected from several of the larger bathymetric depressions in the continental slope of the northern Gulf of Mexico off Texas and western Louisiana from the R.V. *Gyre*. Sediment from the largest and most eastern of these basins was found to have an interstitial fluid containing nearly 150 g of chloride ion per kilogram, almost eight times that of seawater. Although similar hypersaline conditions have been found in samples collected from deep boreholes in the Gulf of Mexico (1) and in bottom waters from three Red Sea basins (2, 3), to our knowledge they have not been previously reported in any open continental shelf or slope environment.

Recently, the R.V. *Gyre* returned to this basin, centered at 26°55′N, 91°20′W (see inset, Fig. 1), in order to define the extent and nature of the brine conditions. A depression containing a pool of anoxic and hypersaline water which approaches the Red Sea brine in total salinity and which is at least three times greater in volume (2, 3) was mapped and sampled in detail. This initial report on a unique marine feature—tentatively named Orca Basin—presents the bathymetric, hydrographic, and seismic description of this basin as well as the bulk chemical composition of its brine.

Orca Basin is an intraslope depression situated within the complex described by Lehner (4) as "the growing margin of the Gulf Coast geosyncline." The complex bathymetry of the slope area has been attributed to salt diapirism and resulting slump features. The recovery of salt from boreholes drilled on several prominent highs along the slope (as close as 60

km northeast of Orca Basin) has provided positive evidence for its occurrence in this region (4).

The basin is a 25-km-long, elbow-shaped depression encompassing an area of approximately 400 km². The enclosing slopes drop from an average depth of 1800 m to a maximum depth of 2400 m within two separate areas. The bathymetry of the basin is depicted in Fig. 1, based on an average sound velocity of 1498 m/sec computed from collected hydrographic data (5). The track lines made in this survey allowed definition of encircling slopes ranging from 3° to a maximum of 14° along the basin perimeter. The strong irregularities in the shape of the feature are typical of the diapiric, salt-induced geomorphology of the continental slope in this area. Numerous diffraction patterns appearing on the bathymetric records are indicative of the locally complex topography.

A minisparker (20-tip, 700-joule) was operated during the survey to obtain shallow seismic data (6). Figure 2 shows a typical sparker line across the basin, revealing up to ½ second of layered reflectors running longitudinally within the basin. Seismically amorphous zones and hyperbolic reflectors to the east and west of the central portion of the basin appear to be the result of sediment slumping along its slopes. However, no positive seismic evidence was found to confirm or negate the presence of massive salt in surface or subbottom sediments.

A midwater sound reflector, similar to those observed during investigations of the Red Sea brines (7), is seen on the sparker profiles (Fig. 2) as a single low-frequency (200- to 300-hertz) reflector within the basin. No reflectors indicative of the brine-seawater interface were seen on either 12-khz or 3.5-khz echo-sounding equipment. An acoustic reflection from such an interface is a function of the resolution of the seismic system employed; thus, observation of a gradual density change at the interface requires the long wavelength provided by a sparker system. Having a "real-time" picture of the brine-seawater interface proved an invaluable sampling aid during the cruise and allowed easy delineation of the lateral extent of the brine (Fig. 1).

Three hydrographic profiles were established across the seawater-brine interface at the locations shown in Fig. 1, using 20-bottle Nansen casts with a Benthos pinger and standard shipboard analytical procedures (8). Data from all three stations are plotted in Fig. 3 as ver-

Table 1. Major chemical composition of brine from Orca Basin compared to average seawater and Red Sea brine. Abbreviations: S_c and S_g, salinity (see footnotes); $d_{22.5°}$, density at 22.5°C.

Sample	S_c (g/liter)	S_g (g/kg)	Cl⁻ (g/kg)	$d_{22.5°}$ (g/ml)	Na⁺ (g/kg)	K⁺ (g/kg)	Ca²⁺ (g/kg)	Mg²⁺ (g/kg)	SO₄²⁻ (g/kg)	H₂O (g/kg)	Si (μM)	NO₃⁻ (μM)	PO₄³⁻ (μM)	O₂ (ml/liter)
Orca brine	308.5*	258.1†	149.5	1.185	91.5	0.63	1.09	1.05	3.66	741.9	235	0	81.5	0
Average seawater	36.3	35.4	19.4	1.025	10.8	0.40	0.41	1.29	2.72	965.0	25‡	23‡	2.5‡	4–5
Red Sea brine§	317.1*	256.4‖	155.3	1.199	92.9	2.16	4.71	0.81	0.75	743.9	235	0.8		0

*Determined aboard ship by conductive salinometer on samples diluted volumetrically to near-seawater conductance. †Determined in the laboratory by conductive salinometer on a gravimetrically diluted sample. ‡In water from 1900 m at the Orca Basin site. §From Brewer et al. (2). ‖Determined by the gravimetric method of Morris and Riley [see (13)].
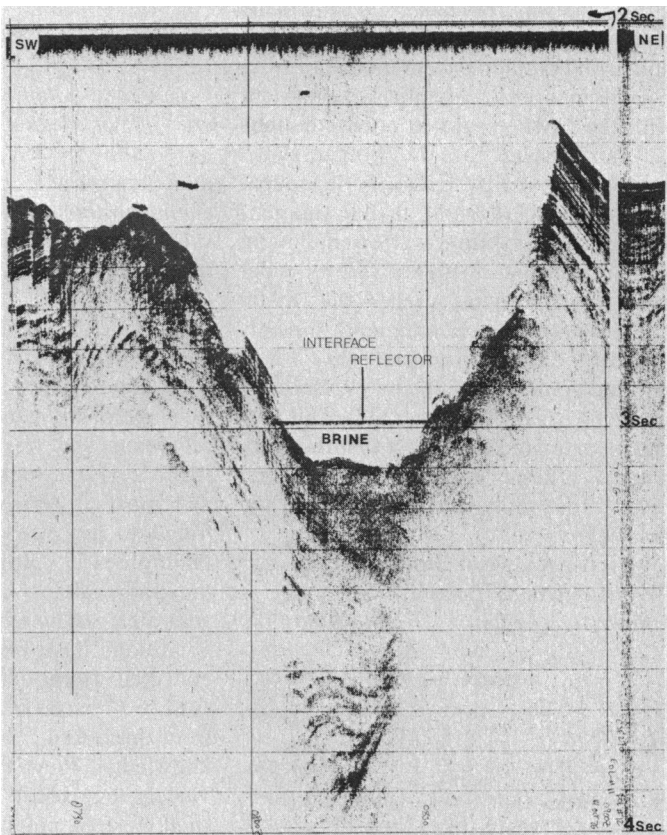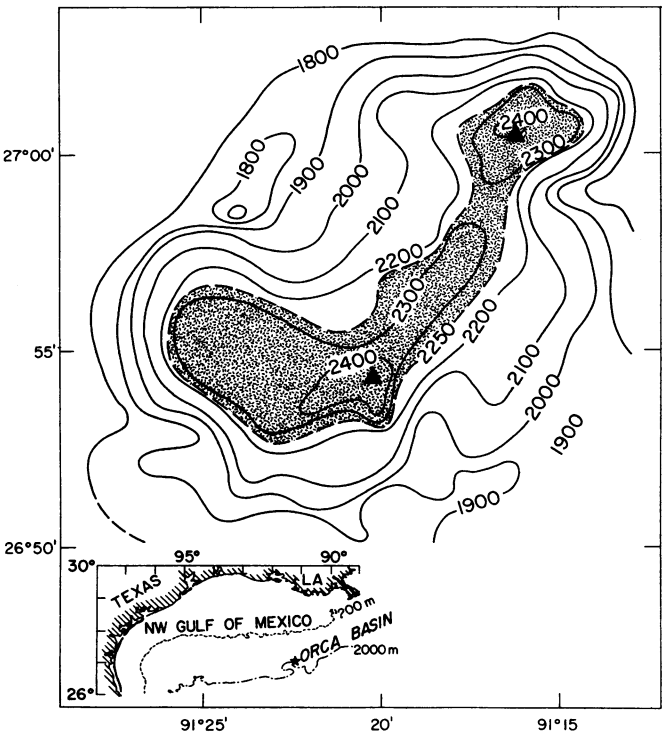

Fig. 1 (left). Bathymetric description and location of the Orca Basin on the northern Gulf of Mexico continental slope (5). Included are the areal extent of the brine (stippled region) and the locations of hydrographic stations 3b, 3c, and 3c-2 (triangles). Fig. 2 (right). Minisparker line along the longitudinal axis of the Orca Basin showing subbottom and midwater seismic reflectance layers (6).

tical profiles with depth. It should be noted that the "salinities" are apparent values determined with a Plessy conductive salinometer, using volumetrically diluted samples compared to standard seawater. Brewer et al. (2) discuss the interpretation of shipboard determination of salinity for the Red Sea brines and make the important point that such solutions are so geochemically different from seawater that only approximate hydrographic comparison can be made to normal oceanic standards.

The obvious feature displayed by all six hydrographic parameters is the sharp interface approximately 200 m above the bottom. The controlling parameter is the increase in total dissolved solids and the resulting density gradient. The effect of this ultrastable condition is to limit vertical exchange to such an extent that (i) the entrained oxygen and nitrate are depleted by organic degradation, (ii) phosphate levels increase from remineralization of organic phosphorus under anoxic conditions, (iii) silica levels increase from water column dissolution of diatom frustules or diffusion upward from the bottom sediments, and (iv) temperature increases because of geothermal warming (9) or heat brought in with the brine.

Table 1 compares the bulk chemical composition of the Orca brine with the composition of average seawater and of the Red Sea brine. Chloride was determined by Mohr titration with silver nitrate (10), sulfate by barium sulfate gravimetry (10), and all the cations by atomic absorption spectrometry (AAS), using a Jarrell-Ash model 810 instrument. The sum of the magnesium and calcium determined by AAS was 168.2 meq/liter, which compares well with the 169.2 meq/liter found by an EDTA total hardness titration (10). The nutrients were determined with a Technicon AutoAnalyzer by standard techniques, and oxygen was determined by the Winkler method (8). The mass sum of the cations and anions determined is approximately 250 g/kg rather than the 258.1 g/kg reported for salinity; the ~ 3 percent discrepancy is attributed to the difference in ionic composition between the brine and the conductometric standard (normal seawater). The cationic and anionic species as determined (Table 1) are balanced as to charge equivalents within the error of analysis.

Craig (11) concluded that the Red Sea brine is formed when seawater circulates through subbottom evaporite deposits, obtaining geothermal heat and dissolved solids before surfacing in the depressions of the central Red Sea. He attributes the near-stoichiometric depletion of magne-

sium and sulfate to selective membrane filtration as the solution percolates through clays, primarily because data on the per mil enrichment in ^{34}S ($\delta^{34}S$) do not indicate any fractionation steps in the sulfate depletion mechanism. In the Orca brine, however, we find no evidence of sulfate depletion and only a slight decrease in Mg^{2+}. Also, the other cations, with the exception of Na^+, increase by a much smaller degree than in the Red Sea, and the temperature increase is comparatively minor. These data and their comparison to the data from the Red Sea suggest to us that the mode of origin for the Orca brine is dis-

solution of a near-surface salt deposit. This conclusion is based primarily on the very small increase in temperature compared to the large increase in dissolved solids, and is supported by the small increase in K^+ and Ca^{2+} relative to Na^+—not very different from the solution that would result from dissolving halite in seawater to near-saturation. In addition, the interstitial water collected during the November 1975 cruise was found to have a dissolved chloride gradient decreasing with depth in the sediment column from the surface. It would appear, then, that the Orca brine was not formed by diffusion from the immediately underlying
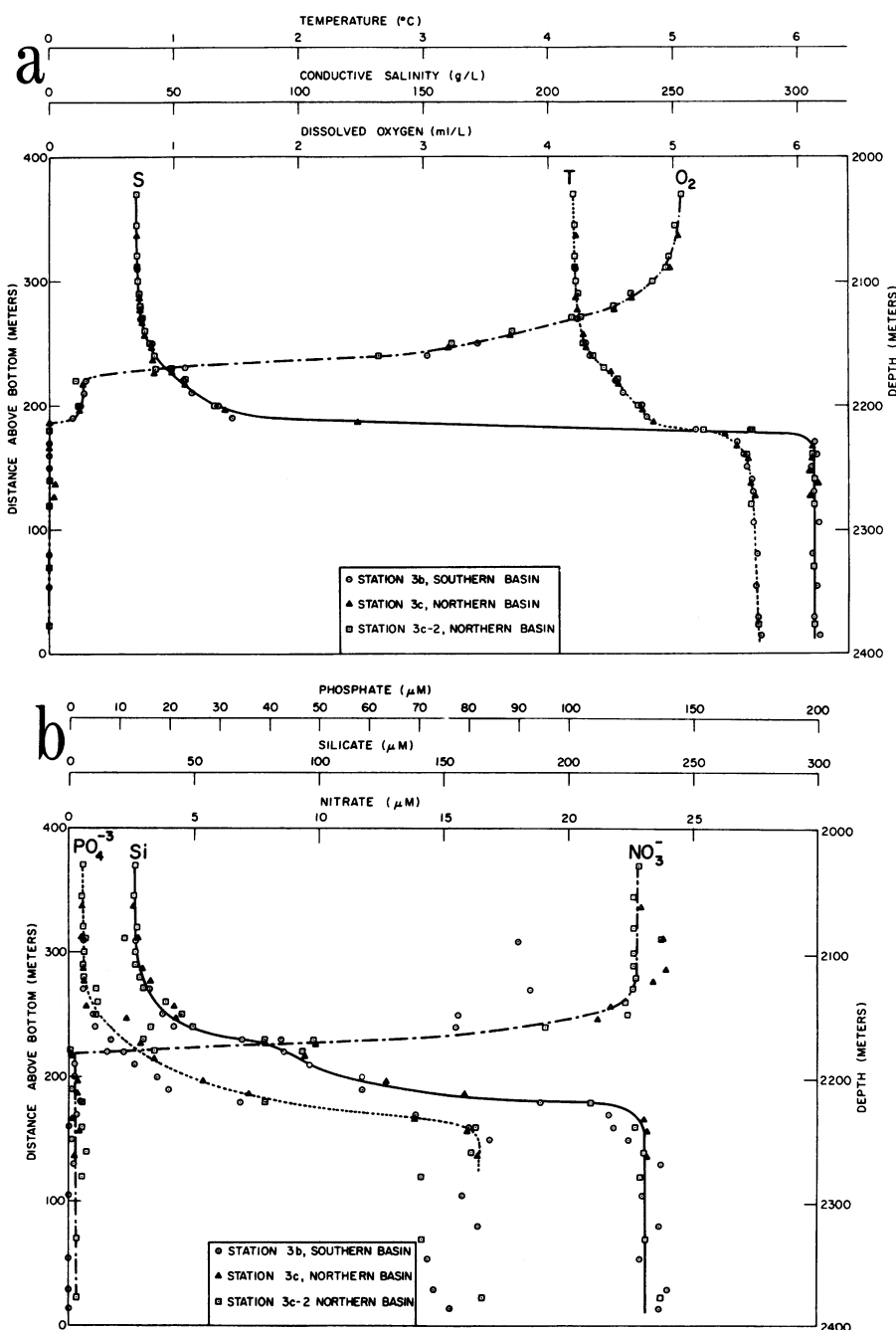

Fig. 3. Vertical profiles of (a) temperature, shipboard conductive salinity, and dissolved oxygen and (b) dissolved phosphate, silicate, and nitrate across the seawater-brine interface for three stations (3b, 3c, and 3c-2) in the Orca Basin. Salinity determinations are discussed in the text.

sediments, but came from some point on the surrounding basin slope.

The existence of the Orca brine in an open continental slope setting is a phenomenon that can provide an in situ laboratory for testing and developing physical and geochemical models, and its availability and ease of sampling should facilitate future work in these areas. Recent articles on the long-range potential of salt gradients for use in both electrochemical concentration cells and osmotic pumps as energy sources (12) indicate a potential economic importance for the Orca brine. Furthermore, it is possible that similar conditions exist in other areas of the northern Gulf of Mexico or elsewhere in the world's oceans. Efforts to locate such occurrences could be greatly aided by use of the seismic technique employed in this study.

ROBERT F. SHOKES*
PETER K. TRABANT
BOB J. PRESLEY
Department of Oceanography,
Texas A&M University,
College Station 77843
DAVID F. REID
Code 334, Naval Ocean
Research and Development Activity,
Bay St. Louis, Mississippi 39520

References and Notes

1. F. Manheim and J. Bischoff, *Chem. Geol.* **4**, 63 (1969).
2. P. Brewer, C. Densmore, R. Munns, R. Stanley, in *Hot Brines and Recent Heavy Metal Deposits in the Red Sea*, E. Degens and D. Ross, Eds. (Springer-Verlag, New York, 1969), pp. 138–147.
3. D. Ross, in *ibid.*, pp. 148–152.
4. P. Lehner, *Am. Assoc. Pet. Geol. Bull.* **53**, 2431 (1969).
5. The bathymetric survey was performed at a frequency of 12 khz and recorded on a 19-inch precision fathometer at a sweep rate of 2 seconds.
6. Sparker data was filtered to a band pass of 300 to 800 hertz and recorded at a 2-second sweep.
7. D. Ross, E. Hays, F. Allstrom, in *Hot Brines and Recent Heavy Metal Deposits in the Red Sea*, E. Degens and D. Ross, Eds. (Springer-Verlag, New York, 1969), pp. 82–97; G. Dietrich and G. Krause, in *ibid.*, pp. 10–14.
8. J. Strickland and T. Parsons, *A Practical Handbook of Seawater Analysis* (Fisheries Research Board of Canada, Ottawa, 1968).
9. The heat needed to raise the temperature of the 40 km³ of brine could be added in about 325 years, assuming an average oceanic geothermal heat flow (1 μcal cm^{-2} sec^{-1}).
10. A. Vogel, *Quantitative Inorganic Analysis* (Wiley, New York, 1968).
11. H. Craig, in *Hot Brines and Recent Heavy Metal Deposits in the Red Sea*, E. Degens and D. Ross, Eds. (Springer-Verlag, New York, 1969), pp. 208–242.
12. B. Clampitt and F. Kiviat, *Science* **194**, 719 (1976); R. Norman, *ibid.* **186**, 350 (1974); O. Levenspiel and N. de Nevers, *ibid.* **183**, 157 (1974); H. Gregor, *ibid.* **185**, 101 (1974); O. Levenspiel and N. de Nevers, *ibid.*, p. 102.
13. A. Morris and J. Riley, *Deep Sea Res.* **11**, 899 (1964).
14. We thank D. R. Schink, M. R. Scott, and J. H. Trefry for helpful discussion and critical review of this manuscript, and the Office of Naval Research and the National Science Foundation for financial support.
* Present address: Science Applications, Inc., 1200 Prospect Street, LaJolla, Calif. 92038.

6 December 1976; revised 26 January 1977

Desert Varnish: The Importance of Clay Minerals

Abstract. *Desert varnish has been characterized by infrared spectroscopy, x-ray diffraction, and electron microscopy. It is a distinct morphological entity having an abrupt boundary with the underlying rock. Clay minerals comprise more than 70 percent of the varnish. Iron and manganese oxides constitute the bulk of the remainder and are dispersed throughout the clay layer.*

Desert varnish is a dark, manganese- and iron-rich coating up to 100 μm thick, which occurs on exposed rock surfaces in dry regions. Associated with this dark coating is an orange coat, which develops in contact with soil on the bottom of desert pavement stones. Detailed physical descriptions of these phenomena are found elsewhere (1).

Desert varnish is important not only for its widespread occurrence and, at times, striking appearance, but also for its possible application to relative age dating. Previous studies have been concerned with field observations, bulk chemistry, and chemical variation within the varnish (1–3), yet the mechanism of varnish formation remains uncertain, and it is still not possible to use varnish with confidence for dating (4). The detailed mineralogical and structural information on which formation theory and dating techniques might be reliably based is unavailable. This report presents the results of the application of infrared spectroscopy, x-ray diffraction, and electron microscopy to such a mineralogical and structural characterization of desert varnish.

We collected varnished rocks of diverse lithology from localities in the Mojave Desert, California, which were previously studied in detail (1). Milligram quantities of varnish were scraped from the rock surface with a tungsten needle under × 20 magnification. A comparison of the infrared patterns of varnish and of its underlying rock indicates a minimum sample purity of 93 percent, based on the intensity of quartz bands near 800 cm^{-1}. Samples for in situ examination were millimeter-sized chips broken from larger samples and examined at × 40 to ensure an undisturbed surface.

Sheet silicate absorption dominates the infrared spectra of desert varnish. The spectra of the black and orange coats shown in Fig. 1 are representative
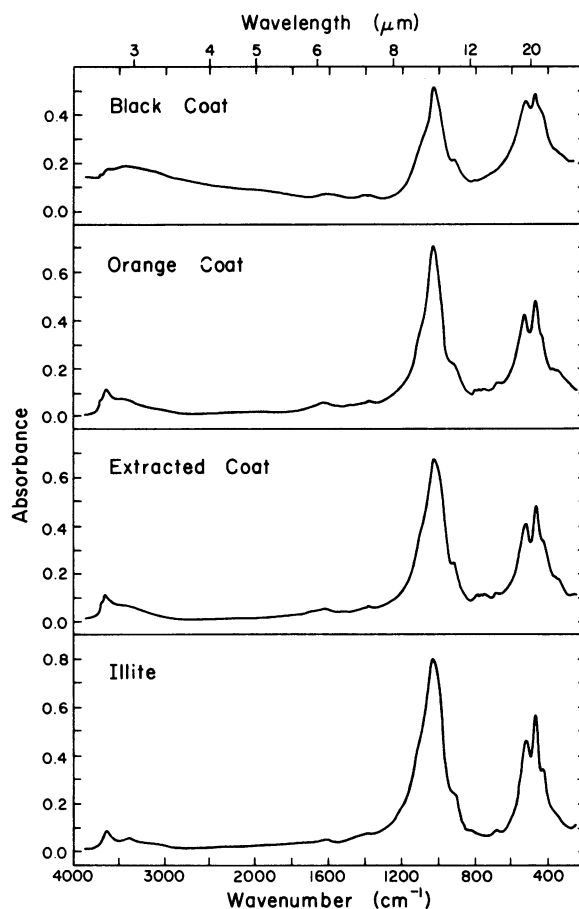
Fig. 1. Infrared spectra of desert varnish showing major features attributable to clay minerals. The spectrum of an illite standard (16) is included for comparison. A 0.5-mg portion of powdered sample was dispersed in a 200-mg KBr pellet, 13 mm in diameter, which was heated to 100°C under vacuum to remove water adsorbed on the KBr.